

Figure S1. PM exposure triggers allergic anti-inflammatory cytokines infiltration in an AED mouse model. (A) Immunofluorescence staining for TNF- α in cornea in naive, OVA and OVA+PM exposed groups. (B) Immunofluorescence staining for IL-4 in cornea in naive, OVA and OVA+PM exposed groups. (C) Changes in the positive area of TNF- α in cornea. (D) Changes in the positive area of IL-4 in cornea. White rectangles indicate TNF- α and IL-4 in cornea; shown in higher-power fields. The scale bar is indicated by a white bar in the lower right corner. In (C and D) data are presented with bar graph with mean \pm SEM ($n = 5$, * $p < 0.05$, ** $p < 0.01$, *** $p < 0.001$, significant difference by one-way ANOVA followed by the Tukey test).

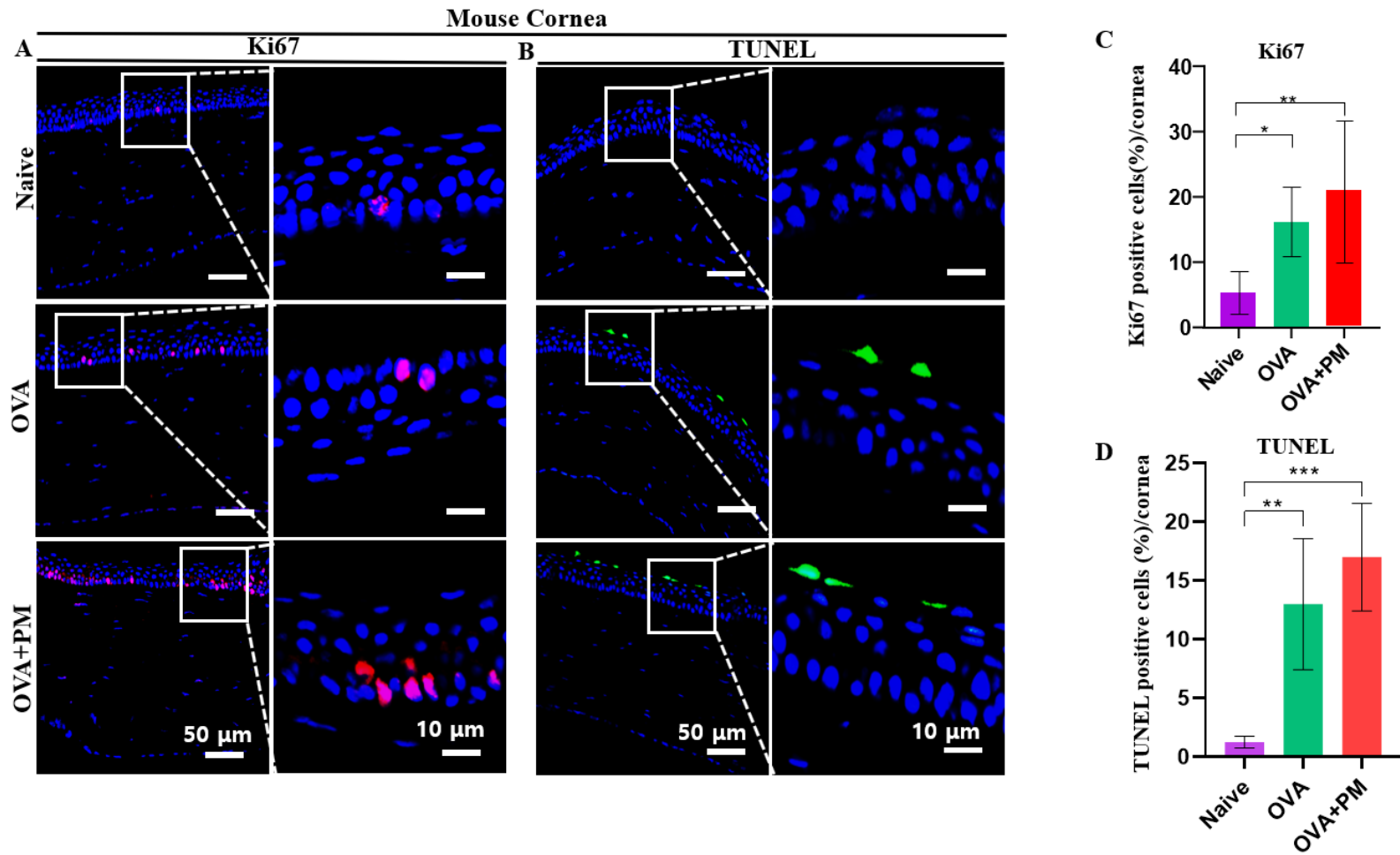


Figure S2. Exposure of PM effects on elevated cell proliferation and cellular apoptosis in an AED mouse model. (A) Immunofluorescence staining for Ki67 in cornea in naive, OVA and OVA+PM exposed groups. (B) TUNEL staining for cellular apoptosis in cornea in naive, OVA and OVA+PM exposed groups. (C) Changes in the ki67 positive cells in cornea. (D) Changes in the TUNEL positive cells percentage in cornea. White rectangles indicate the ki67 and TUNEL positive cells cornea showing in higher-power fields. White rectangles indicate the ki67 and TUNEL positive cells in cornea; shown in higher-power fields. The scale bar is indicated by a white bar in the lower right corner. In (C and D) data are presented with bar graph with mean \pm SEM ($n = 5$, * $p < 0.05$, ** $p < 0.01$, *** $p < 0.001$, significant difference by one-way ANOVA followed by the Tukey test).

